ELECTRONIC SUPPLEMENTARY INFORMATION (ESI)

Spectral Characterization and Surface Complexation Modeling of Low Molecular Weight Organics on Hematite Nanoparticles: Role of Electrolytes in the Binding Mechanism

Arthur Situm[a], Mohammad A. Rahman[a], Sabine Goldberg[b], and Hind A. Al-Abadleh[a]*

[a]Department of Chemistry and Biochemistry, Wilfrid Laurier University,

Waterloo, ON N2L 3C5, Canada

[b]USDA-ARS, U.S. Salinity Laboratory, Riverside, CA 92507, USA

Journal: Environmental Science: Nano

Prepared: June 17, 2016

Content (16 pages):

1. TEM images and zeta potential measurements of hematite nanoparticles

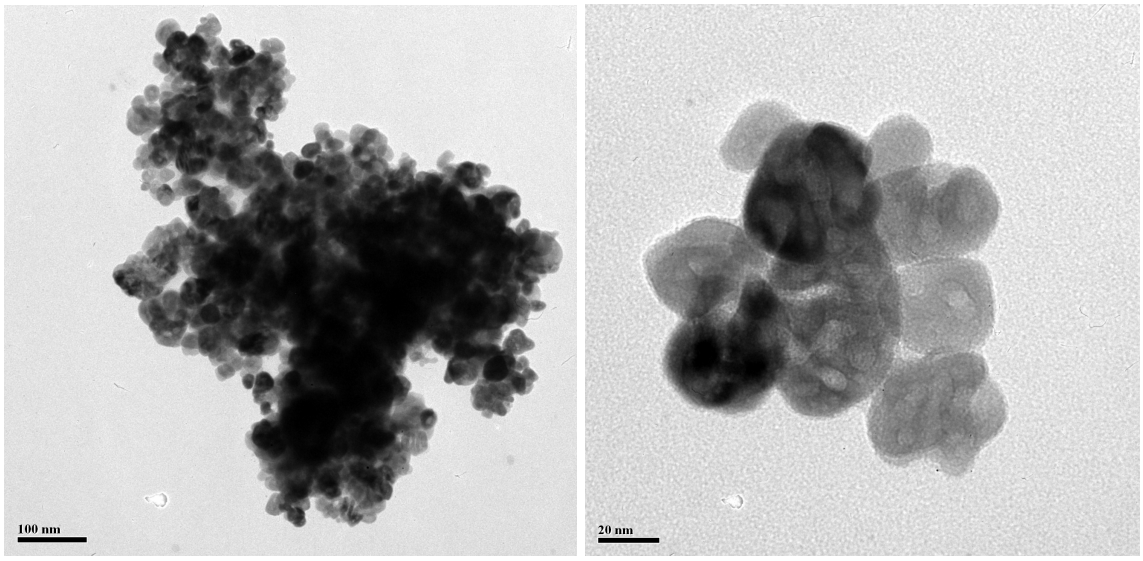

Fig. S1: Representative TEM images of hematite nanoparticles collected using Philips CM12 electron microscope operated at 120 keV. The particles were suspended in ethanol and a drop placed on holey carbon-coated Cu grid, which was dried before the TEM analysis.

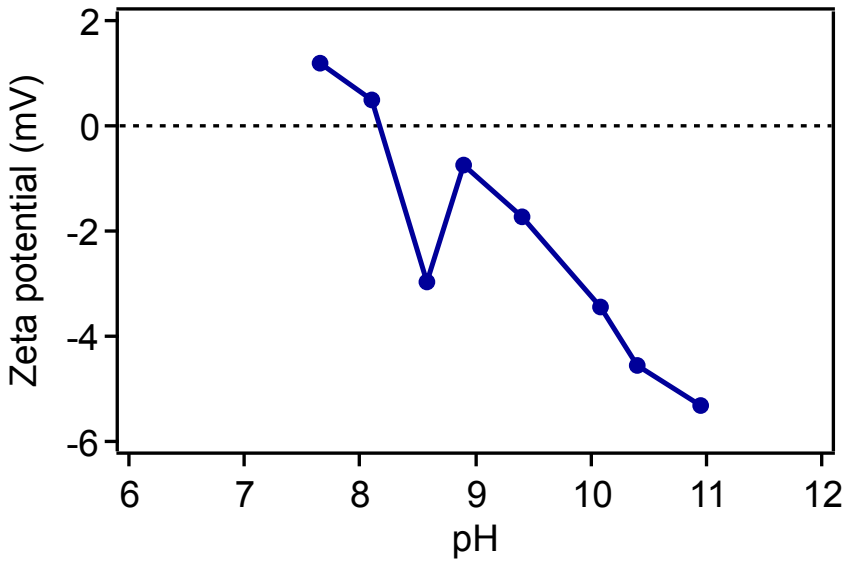

Fig. S2: Titration of 1% aqueous solution hematite nanoparticles with 0.1 N sodium hydroxide (NaOH). The iso-electric point is the pH at which the zeta potential is 0 mV. The pH of this solution was adjusted to 7.65 with 3 drops of 1 N HCl. The iso-electric point of this material was determined to be 8.45. No organic molecules were in solution.

2. Calculations of surface coverage on porous hematite nanoparticle films from ATR-FTIR spectra and Table S1

To quantify the relative equilibrium surface coverage by a particular organic as a function of concentration, baseline-corrected ATR absorbances [i.e., peak height at a given wavenumber, $A(\tilde{\nu})$] of spectral features assigned to surface complexes were used. Values of $A(\tilde{\nu})$ were obtained using the height tool in OMNIC software that runs the FTIR spectrometer relative to the absorbance at 2000 cm^{-1}, which has no IR signals from any of the species used in our studies. The derivation of equation S1 for estimating the surface coverage was reported earlier (see reference [1]):

$$S(\text{molecules}\cdot\text{cm}^{-2}) = \frac{A(\tilde{\nu})}{\varepsilon(\tilde{\nu})N^2 d_p(\tilde{\nu})\rho_b \cdot S.A._{BET}} \quad \text{(S1)}$$

where:

- $\varepsilon(\tilde{\nu})$ is molar extinction coefficient of the adsorbate in $cm^2\cdot molecule^{-1}$ (listed in Table S1 for each organic compound, which was obtained from the Beer's plot of aqueous phase standard solutions at pH 7 using a calculated effective pathlength at a given $\tilde{\nu}$ for water as the sample),
- N is the total number of reflections inside the IRE (equals 4.8 for our ATR IRE with effective angle of incidence $\theta = 64.4°$ using the optical properties of liquid water as described in the Supporting Information of reference [2]),
- d_p is the depth of penetration per reflection in cm after accounting for porosity (see below), which approximately equals to d_e/N, and calculated using $\lambda/[2\pi n_1\sqrt{\sin^2\theta-(n_2/n_1)^2}]$, λ is the wavelength of light ($1/\tilde{\nu}$), n_1 and n_2 are the refractive indices of IRE (2.4 for ZnSe) and the sample, respectively),

- ρ_b is the bulk density of the deposited hematite film (equals 1.1 g/cm^3 as detailed in text), and
- $S.A._{BET}$ is the specific surface area of the hematite particles (equals 5.4×10^5 cm^2/g).

Table S1. Values of the molar extinction coefficients, $\varepsilon(\tilde{\nu})$, used in surface coverage calculations at pH 7

Compound	Wavenumber, $\tilde{\nu}$ (cm^{-1})	d_e (cm)	$\varepsilon(\tilde{\nu})$ (cm^2/molecule)
Citrate (aq)	1570	2.8×10^{-4}	2.1×10^{-18}
Iron(III) Oxalate (aq)	1677	2.6×10^{-4}	3.3×10^{-18}
Pyrocatechol (aq)	1260	3.5×10^{-4}	5.1×10^{-19}

In the presence of a porous hematite film, the value of n_2 has to account for the porosity and the presence of solvent in the pores.[3] A volume-weighed average of the refractive index of the particles (n_2') is calculated using $n_2' = F_v \cdot n_{par} + (1 - F_v) \cdot n_{H_2O(l)}$, where $F_v = \rho_b(gcm^{-3})/\rho_{true}(gcm^{-3})$, n_{par} is the particle refractive index (2.9 for hematite) and $n_{H_2O(l)} = 1.3$.[4] For a 6 mg film hematite, F_v is calculated to be 0.21 using $\rho_{true} = 5.3$ gcm^{-3}. Hence, the value of n_2' is calculated to be 1.6. Using this value for the refractive index of the hematite nanoparticles porous sample in contact with organic solution results in $d_p(\tilde{\nu})$ as reported in Table S2.

Table S2. Values of $d_p(\tilde{\nu})$ used in surface coverage calculations of each organic at pH 7 per eq. (S1)

Compound	Wavenumber, $\tilde{\nu}$ (cm^{-1})	$d_p(\tilde{\nu})$ (cm)
Citrate (ads)	1581	6.9×10^{-5}
Oxalate (ads)	1670	6.6×10^{-5}
Pyrocatechol (ads)	1258	8.7×10^{-5}

3. Surface Complexation Modeling (SCM) for the clean surface and bulk species.

In the present application of the model the following surface complexation constants were considered:

$$\mathrm{FeOH} + \mathrm{H^+} \leftrightharpoons \mathrm{FeOH_2^+} \quad \text{(S2)}$$

$$\mathrm{FeOH} \leftrightharpoons \mathrm{FeO^-} + \mathrm{H^+} \quad \text{(S3)}$$

$$\mathrm{FeOH} + \mathrm{K^+} \leftrightharpoons \mathrm{FeO^-} - \mathrm{K^+} + \mathrm{H^+} \quad \text{(S4)}$$

$$\mathrm{FeOH} + \mathrm{H^+} + \mathrm{Cl^-} \leftrightharpoons \mathrm{FeOH_2^+} - \mathrm{Cl^-} \quad \text{(S5)}$$

where FeOH represents reactive surface hydroxyl groups on hematite. It is model convention to write the reactions starting with the undissociated component FeOH. Equilibrium constant expressions for the surface complexation constants are:

$$\mathrm{K_+(int)} = \frac{[\mathrm{FeOH_2^+}]}{[\mathrm{FeOH}][\mathrm{H^+}]}\exp(\mathrm{F}\psi_o / \mathrm{RT}) \quad \text{(S6)}$$

$$\mathrm{K_-(int)} = \frac{[\mathrm{FeO^-}][\mathrm{H^+}]}{[\mathrm{FeOH}]}\exp(-\mathrm{F}\psi_o / \mathrm{RT}) \quad \text{(S7)}$$

$$\mathrm{K_{K^+}(int)} = \frac{[\mathrm{FeO^- - C^+}][\mathrm{H^+}]}{[\mathrm{FeOH}][\mathrm{C^+}]}\exp[\mathrm{F}(\psi_\beta - \psi_o) / \mathrm{RT}] \quad \text{(S8)}$$

$$\mathrm{K_{Cl^-}(int)} = \frac{[\mathrm{FeOH_2^+ - A^-}]}{[\mathrm{FeOH}][\mathrm{H^+}][\mathrm{A^-}]}\exp[\mathrm{F}(\psi_o - \psi_\beta) / \mathrm{RT}] \quad \text{(S9)}$$

The triple layer SCM parameter values were fixed at: $\log K_+(\mathrm{int}) = 4.3$, $\log K_-(\mathrm{int}) = -9.8$, $\log K_{K+}(\mathrm{int}) = -9.3$, $\log K_{Cl-}(\mathrm{int}) = 5.4$, $C_1 = 1.2$ F m^{-2}, $C_2 = 0.2$ F m^{-2} used previously in our description of organic and inorganic arsenic adsorption.[1,5]

It is also model convention to write the surface complexation reactions starting with the completely undissociated acids as the components. This convention is used

because the use of uncharged species simplifies the species-component matrix for computation. Chemically, completely equivalent formation reactions can be written starting with dissociated acid species because the aqueous acid dissociation reactions are contained in the model. This is similar to solid precipitation reactions, where identical products can be formed from different starting components.

The model application contains the aqueous speciation reaction(s) for oxalic acid (OA), citric acid (CA), and pyrocatechol (PC):

$$H_2OA \leftrightharpoons HOA^- + H^+ \quad \text{(S10)}$$

$$HOA^- \leftrightharpoons OA^{2-} + H^+ \quad \text{(S11)}$$

$$H_3CA \leftrightharpoons H_2CA^- + H^+ \quad \text{(S12)}$$

$$H_2CA^- \leftrightharpoons HCA^{2-} + H^+ \quad \text{(S13)}$$

$$HCA^{2-} \leftrightharpoons CA^{3-} + H^+ \quad \text{(S14)}$$

$$H_2PC \leftrightharpoons HPC^- + H^+ \quad \text{(S15)}$$

$$HPC^- \leftrightharpoons PC^{2-} + H^+ \quad \text{(S16)}$$

The triple layer SCM parameter logK values for the organic acids were fixed at -1.25 and -5.06 for OA, -3.13, -7.89, and -14.29 for CA, and -9.34, and - 21.94 for PC based on their pK_a values.[4]

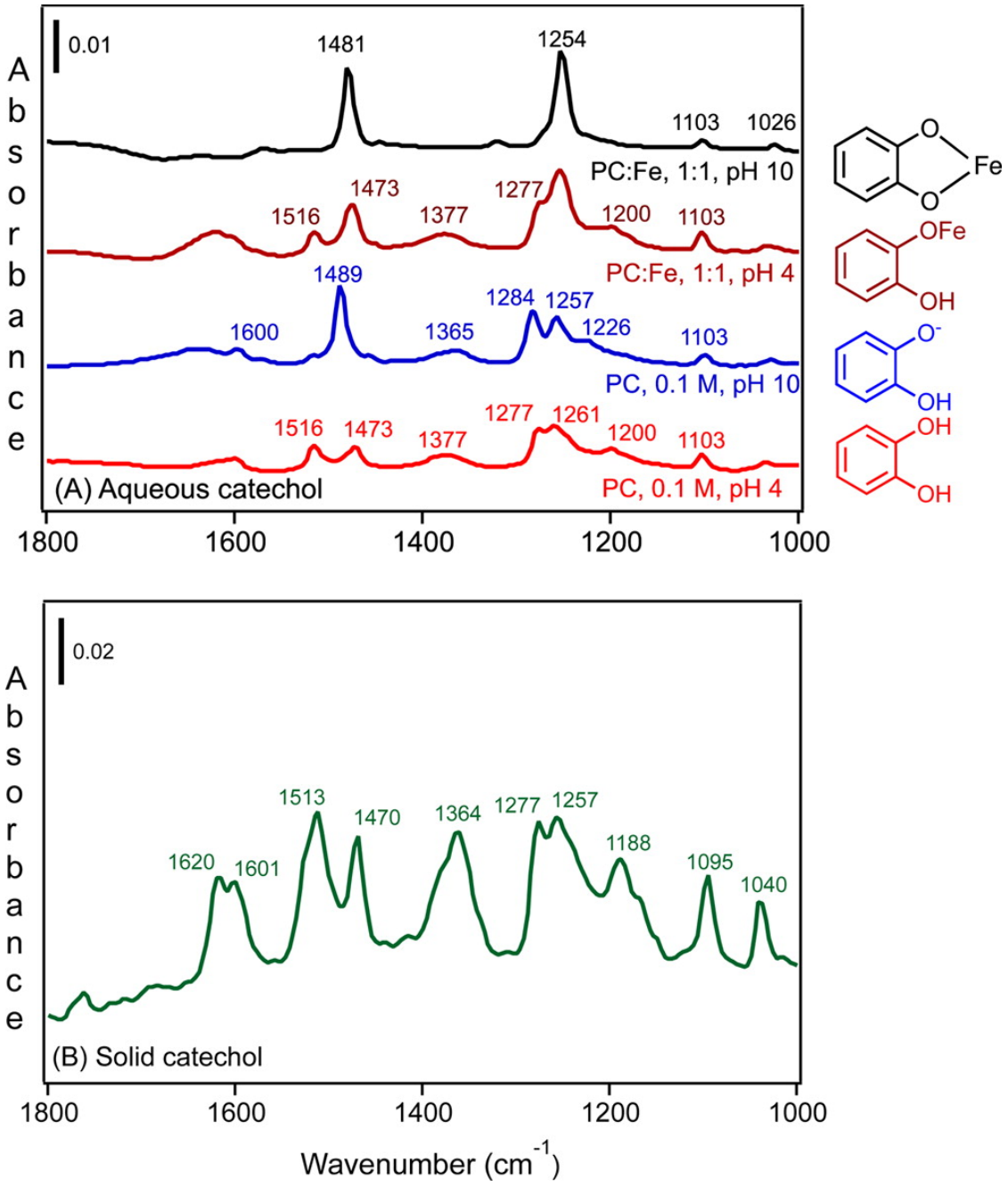

Fig. S3: (A) ATR-FTIR absorbance spectra of 0.1 M aqueous catechol and catechol−Fe complexes (0.2 and 0.1 M for catechol; from bottom) as a function of pH. Ratios listed are mol/mol. (B) DRIFTS absorbance spectrum of 3% solid catechol. PC = catechol. Reprinted with permission from reference [6]. Copyright 2016 American Chemical Society.

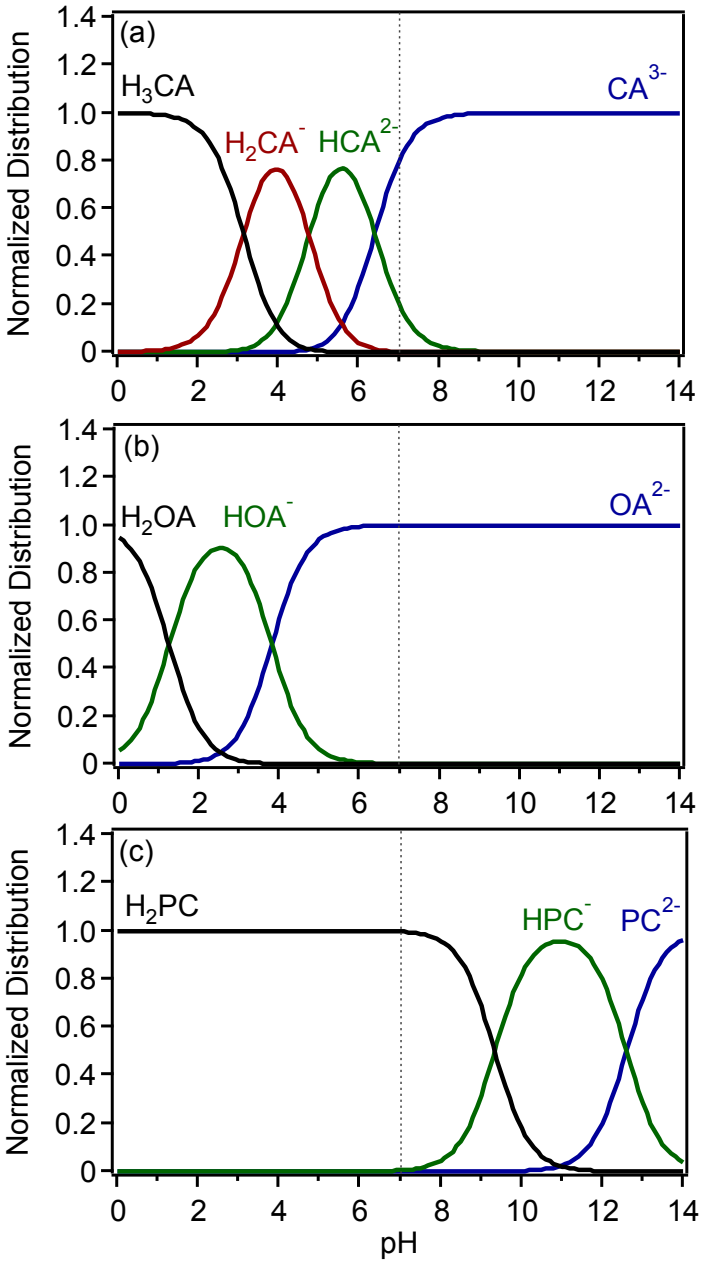

Fig. S4: Normalized distribution curves for the organic compounds used in this study based on their pK_a values[4]: (a) citric acid (CA) at 3.13, 4.76 and 6.40, (b) oxalic acid (OA) at 1.25 and 3.81, and (c) pyrocatechol (PC) at 9.34 and 12.6, respectively.

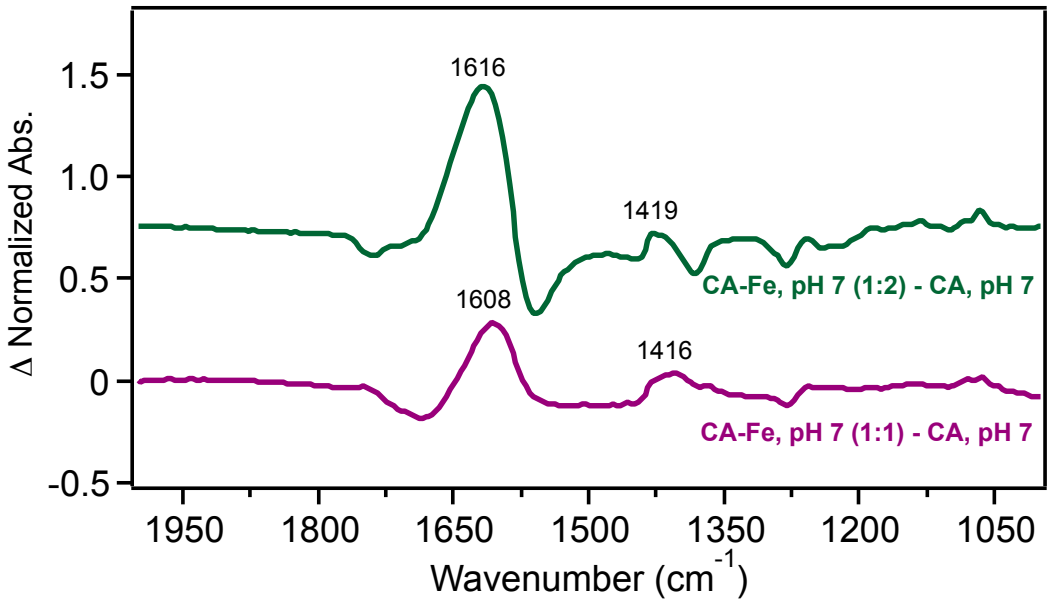

Fig. S5: Difference between normalized spectra collected for citrate complexed to Fe(III) in 1:1 and 1:2 molar ratios and the spectrum collected for uncomplexed citrate at pH 7.

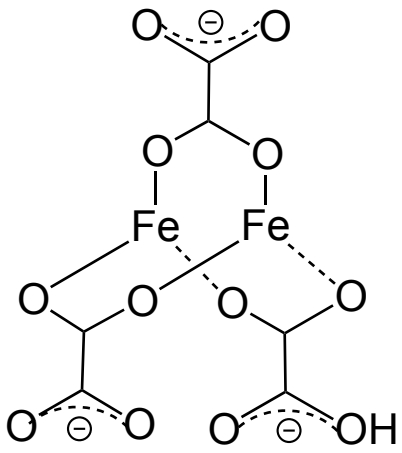

$Fe_2(C_2O_4)_3$ (aq) at pH 7

Fig. S6: Structure of aqueous phase $Fe_2(C_2O_4)_3$ at pH 7 based on spectral analysis and symmetry considerations by Edwards and Russell.[7]

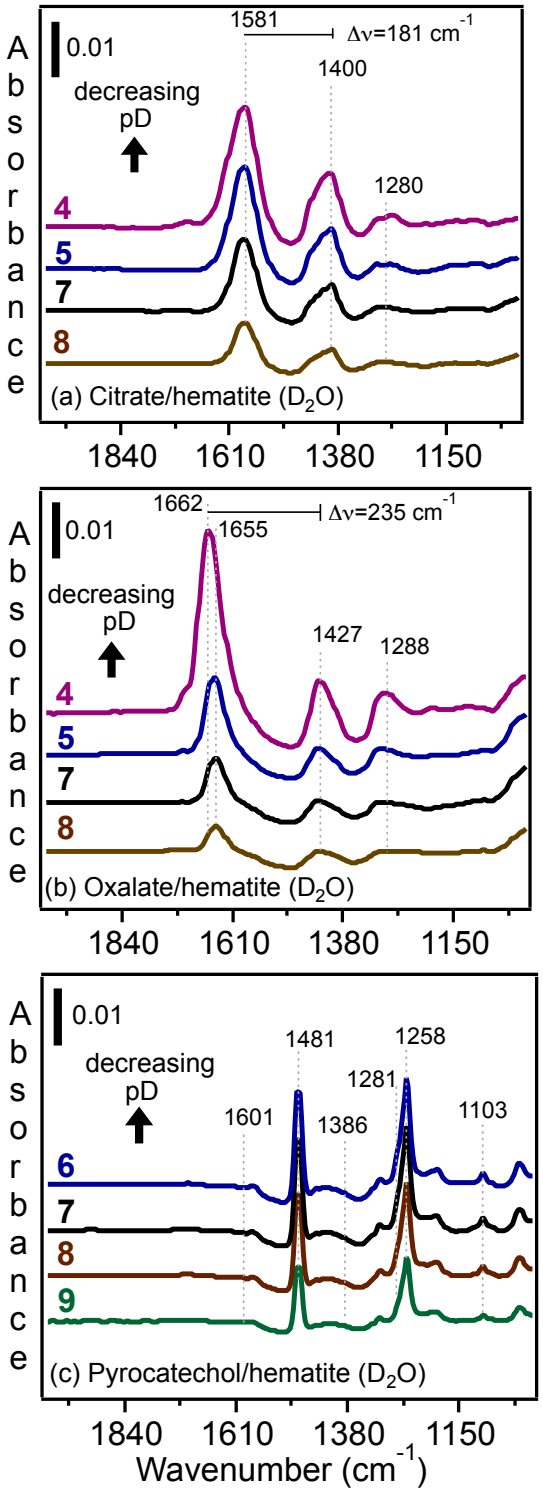

Fig. S7: Representative ATR-FTIR absorbance of adsorbed (a) citrate, (b) oxalate, and (c) pyrocatechol on hematite nanoparticles after flowing 10^{-4} M solutions prepared in D_2O after 10 min flow as a function of decreasing pD from 9 to 5. The electrolyte concentration was 0.01 M KCl, which is 100x higher than [organics(aq)].

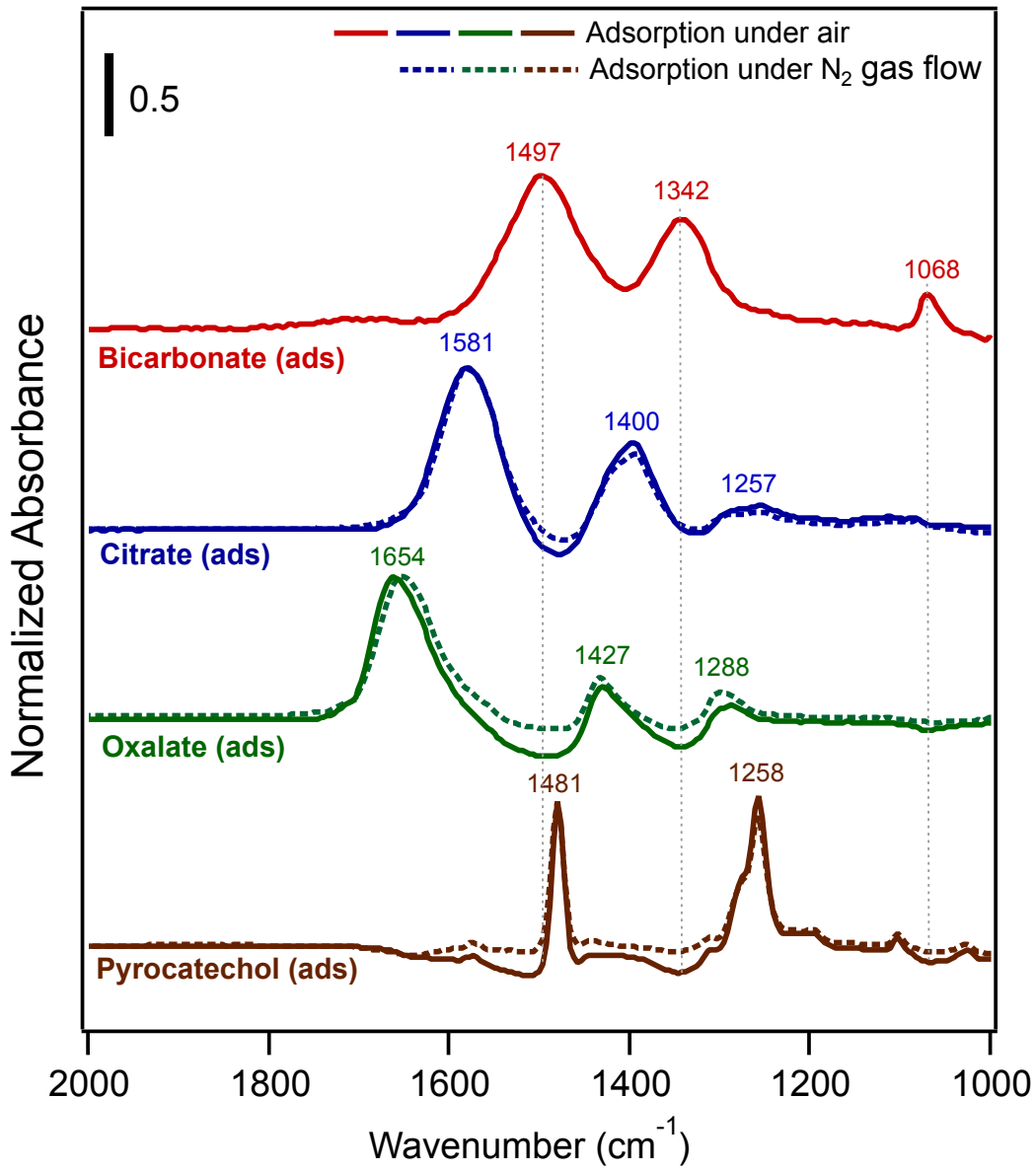

Fig. S8: Normalized ATR-FTIR absorbance spectra of surface species after 30 flow of 1 mM solutions of (from top): sodium hydrogen carbonate, citrate, oxalate and pyrocatechol on hematite nanoparticles at pH 7, under air (solid lines) or continuous flow of N_2 gas in solutions (dashed lines).

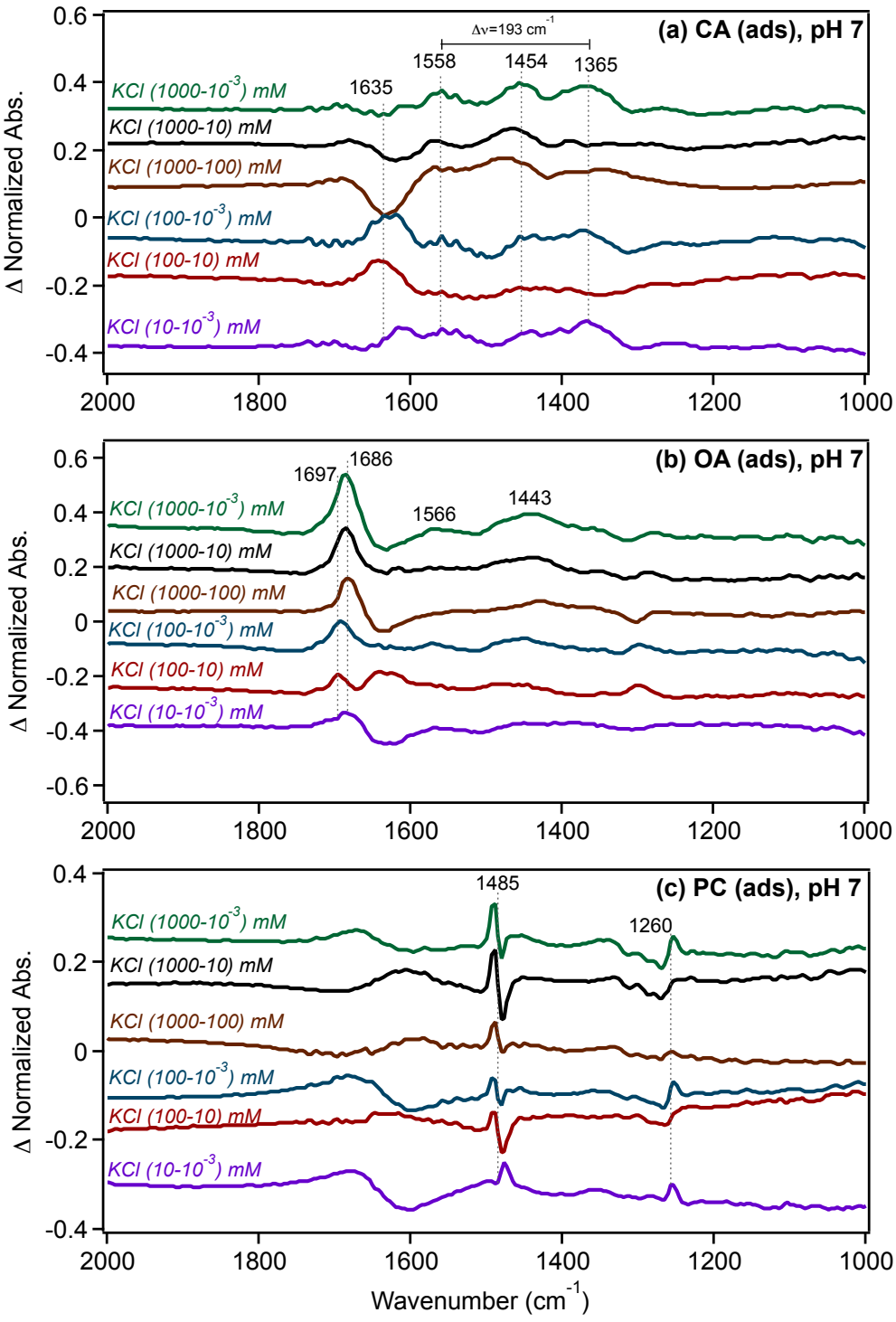

Fig. S9: Difference between normalized spectra collected for adsorbed organics: citrate (CA), oxalate (OA) and pyrocatechol (PC) after 30 min flow at pH 7 time as a function of [KCl(aq)]. Spectra offset for clarity

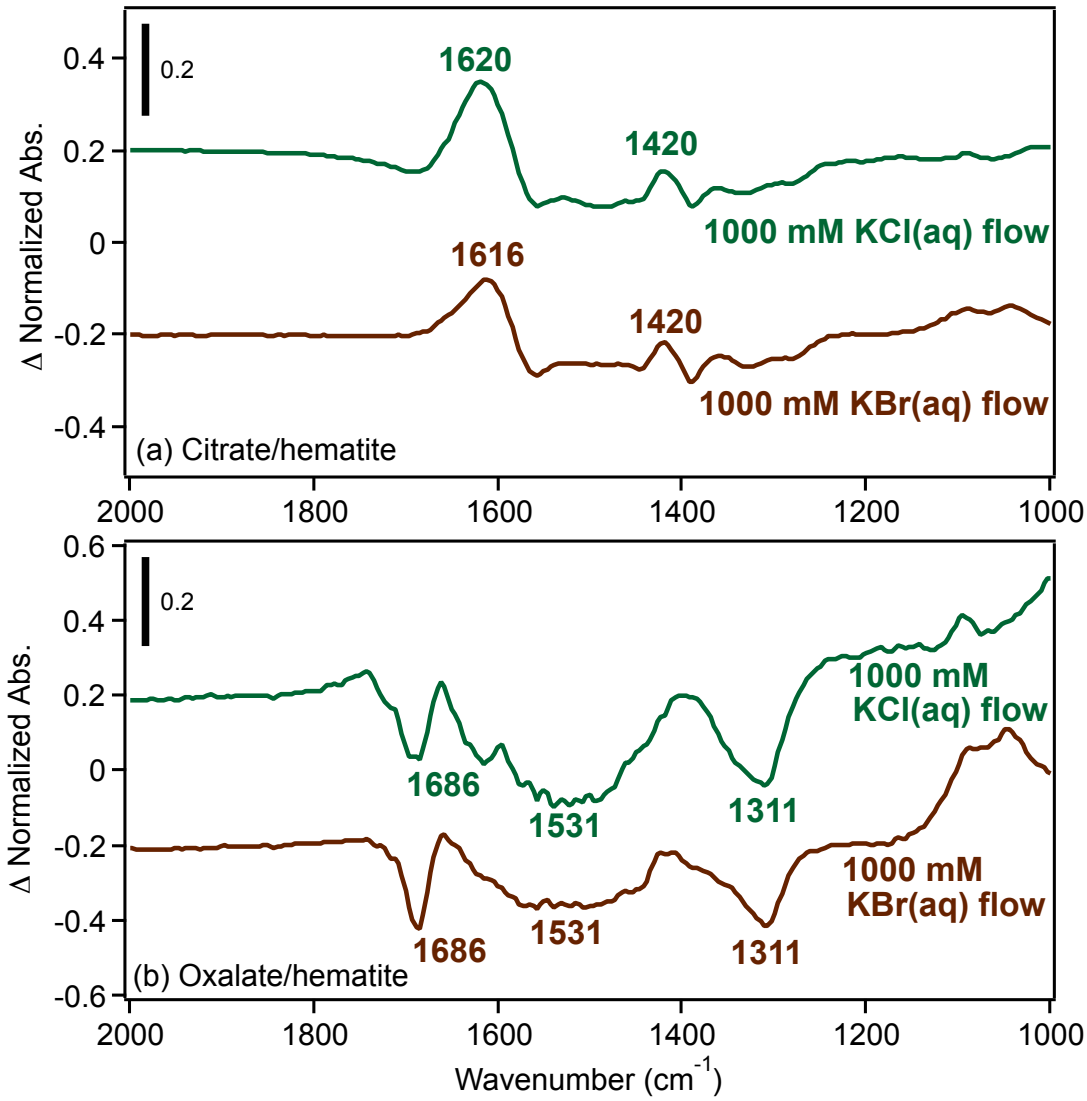

Fig. S10: Difference between normalized spectra collected for adsorbed organics retained by the hematite nanoparticles after 80 min of 1000 mM KCl and KBr at pH 7. Spectra offset for clarity.

References:

1 W. Mitchell, S. Goldberg and H. A. Al-Abadleh, *J. Coll. Inter. Sci.*, 2011, 358, 534-540.

2 S. Depalma, S. Cowen, T. N. Hoang and H. A. Al-Abadleh, *Environ. Sci. Technol.*, 2008, 42, 1922-1927.

3 G. Lefevre, *Adv. Coll. Inter. Sci.*, 2004, 107, 109-123.

4 D. R. Lide, ed., *CRC Handbook of Chemistry and Physics*, Taylor & Francis, Boca Raton, 2012-2013.

5 M. A. Sabur, S. Goldberg, A. Gale, N. J. Kabengi and H. A. Al-Abadleh, *Langmuir*, 2015, 31, 2749-2760.

6 J. Tofan-Lazar, A. Situm and H. A. Al-Abadleh, *J. Phys. Chem. A*, 2013, 117, 10368-10380.

7 H. G. M. Edwards and N. C. Russell, *J. Molec. Struc.*, 1998, 443, 223-231.